Environmental Science and Pollution Research (2021) 28:26828–26839
https://doi.org/10.1007/s11356-021-12545-1

RESEARCH ARTICLE

The in situ catalytic oxidation of sulfamethoxazole via peroxydisufate activation operated in a NG/rGO/CNTs composite membrane filtration

Feiyue Qian[1,2] · Honggui Yin[1] · Feng Liu[1,2] · Jiayi Sheng[1] · Shiqian Gao[1,2] · Yaoliang Shen[1,2]

Received: 22 September 2020 / Accepted: 14 January 2021 / Published online: 26 January 2021

Abstract

Metal-free carbonaceous composite membranes have been proven to effectively drive novel in situ catalytic oxidation for the degradation of organic pollutants via persulfates activation. In this study, nitrogen-doped graphene (NG) was employed as a modifier to enhance the catalytic activity of the carbon mats by assembly with reduced graphene oxide (rGO) and carbon nanotubes (CNTs) on the top of a nylon supporter. The morphology and performance of the NG/rGO/CNTs composite membrane were compared to those obtained without the addition of NG (rGO/CNTs). Owing to the larger nanochannels for water delivery and stronger hydrophobicity on the surface, the NG/rGO/CNTs composite membrane shows a superior low-pressure filtration performance in favor of energy-saving operation. For the in situ catalytic oxidation of the NG/rGO/CNTs composite membrane through the activation of peroxydisufate (PDS), the average removal rate of sulfamethoxazole (SMX), one of frequently detected sulfonamide antibiotics in water, can reach 21.7 $mg{\cdot}m^{-2}{\cdot}h^{-1}$ under continuous filtration mode, which was 17% more rapid than that of the rGO/CNTs, resulting in significant detoxifying of the oxidation intermediates. Owing to the addition of NG into the carbon mats, the reactive nitrogen-doped sites identified by X-Ray photoelectron spectroscopy (XPS), such as pyridinic and graphitic N, played important roles in PDS activation, while both the radical and non-radical pathways were involved in in situ catalytic oxidation. According to the experimental evidence of the effects that solution environment has on the SMX removal and transmembrane pressure, the NG/rGO/CNTs composite membrane shows a relatively high resistance to changes in the solution pH, chloride ion inhibition, and background organics fouling. These results suggest a new approach to the application of activated persulfate oxidation in water treatment, such that improvements to the reaction stability warrant further investigation.

Keywords In situ catalytic oxidation · Peroxydisufate activation · Composite membrane · Nitrogen-doped graphene · Sulfamethoxazole · Solution environment

Introduction

Interest in activated persulfate oxidation based on metal-free carbonaceous materials has increased in the degradation of emerging contaminants in water environments, such as pharmaceuticals and personal care products (PPCPs), due to the high yield of reactive oxygen species (ROS) via various activation methods. Previous studies have shown that external energy activators (e.g., UV irradiation, heat, ultrasound) (Devi et al. 2016; Gao et al. 2020) and homogeneous (e.g., base, quinones, and metal ions) (Fang et al. 2013; Qi et al. 2016; Zhang et al. 2015) and heterogeneous (e.g., metal/metal oxides) (Lei et al. 2015) catalysts exhibit high performance in activating persulfates, including peroxydisufate (PDS) and peroxymonosulfate (PMS), for recalcitrant organics removal. However, there are certain limitations that cannot be ignored in water treatment, such as economic concerns associated with energy consumption, secondary pollution from chemicals addition, and potential ecological risks of metal leaching.

Responsible Editor: Ricardo Torres-Palma

✉ Feiyue Qian
qfywater@163.com

[1] School of Environmental Science and Engineering, Suzhou University of Science and Technology, No. 1 Kerui Road, Suzhou 215009, People's Republic of China

[2] National and Local Joint Engineering Laboratory of Municipal Sewage Resource Utilization Technology, No. 1 Kerui Road, Suzhou 215009, People's Republic of China

To overcome these shortcomings, the application of carbonaceous catalysts provides a metal-free alternative without external energy inputs. Compared with carbonaceous catalysts in bulk (e.g., activated carbon, biochar, and carbon fiber), nanocarbon materials (e.g., carbon nanotubes (CNTs), graphene-based materials, and mesoporous carbon) have simplified configurations with abundant accessible active sites, such that they are regarded as a better candidate to efficiently drive activated persulfate oxidation via radical and non-radical pathways (Chen et al. 2018; Yu et al. 2020a). The radical pathway is based on electron transfer for the activation of the peroxide bond (O–O) in persulfates to produce sulfate radical ($SO_4^{\cdot-}$), hydroxyl radical (HO·), and superoxide radical ($O_2^{\cdot-}$) for organic oxidation, in which $SO_4^{\cdot-}$ (E_0 = +2.5–3.1 V vs NHE) has a significantly longer lifetime, i.e., $t_{1/2}$ = 30–40 μs, than HO·, i.e., $t_{1/2} \leq 1$ μs, favoring excellent one-electron oxidation (Liu et al. 2020; Matta et al. 2010). In contrast, the non-radical pathway is considered a surface-confined reaction to produce ROS with a relatively moderate oxidative potential, including surface-bound $SO_4^{\cdot-}$, reactive carbon-persulfates complexes, singlet oxygen ($^1O_2$), and electron transfer, which shows selective reactivity toward electron-rich substances and has a high resistance to the influences of radical scavengers (Cheng et al. 2019; Guan et al. 2017; Yu et al. 2020b).

Recently, a hybrid system combining activated persulfate oxidation and graphene-based membrane filtration, known as in situ carbonaceous catalytic oxidation, was developed for water treatment in a continuous operation mode. In comparison with conventional suspension reaction systems, the primary advantage of in situ catalytic oxidation is the absence of an additional solid-liquid separation procedure after treatment, which avoids the inadvertent release of nanocarbon materials into the environment. In our recent study, a catalytic composite membrane was prepared by assembling reduced graphene oxide (rGO) with CNTs on the top of a nylon microfiltration membrane via vacuum filtration, which was verified to be highly efficient in activating PDS for the degradation of sulfamethoxazole (SMX) from water within a short contact time (t_c < 1 s) of the carbon mats (Sheng et al. 2020). In an earlier report by Liu et al. (2016), the oxidation rate of target phenol compounds was significantly accelerated by enhancing mass transfer in the graphene-based filtration, as compared with the batch system.

In addition, nitrogen (N) doping can greatly improve the catalytic activity of graphene derivatives, as the introduction of nitrogen atoms can tailor the local electronic structure of neighbors sp^2 carbon to cause persufate activation and/or create Lewis basic sites to coordinate a redox process (Chen and Carroll 2016; Duan et al. 2015b; Ren et al. 2020). So far, there have been a few attempts employing N-doped graphene derivatives for the modification of catalytic membranes for the degradation of organic pollutants (Pedrosa et al. 2019; Vieira et al. 2020), but more experimental evidence with respect to process optimization and solution environment effects are required for the application of in situ catalytic oxidation in water treatment.

In this study, SMX was used as the target organic compound in an aqueous solution, which is one of the widely used sulfonamide antibiotics in human and animal medicines, is frequently detected in natural environments, and has chronic effects on aquatic organisms (Guan et al. 2019; Isidori et al. 2005). To develop a novel metal-free catalytic membrane, commercial N-doped graphene (NG) was employed as the modifier to fabricate the NG/rGO/CNTs composite membrane. First, the surface morphology and filtration performance of the NG/rGO/CNTs composite membrane were characterized and compared with the rGO/CNTs reported in our recent report. Second, the in situ catalytic oxidation based on PDS activation for the removal of SMX was conducted under continuous and circulating filtration modes, demonstrating the advantages of the NG/rGO/CNTs composite membrane at efficient SMX degradation, energy savings for operation, and the detoxification of oxidation intermediates. Finally, the influences that solution environment, including the solution pH, chloride ion (Cl^-), and background organics, have on the oxidation of SMX were evaluated, providing desirable explanations of the reaction mechanisms involved in systems.

Materials and methods

Chemicals and materials

SMX (CAS 723-46-6, > 98% purity, Molecular weight 253.28 Dalton) and sodium peroxydisufate ($Na_2S_2O_8$, CAS 7775-27-1, ≥ 99% purity) were purchased from Sigma-Aldrich Co. (USA). Fulvic acid (FA, CAS 1415-93-6, >90% purity, Molecular weight 227.17 Dalton) and tannin acid (TA, CAS 1401-55-4, >98% purity, Molecular weight 1701.20 Dalton) as model natural organic matter (NOM) were obtained from Shanghai Macklin Biochemical Co., Ltd (China). All other chemicals were of analytical grade or better.

The commercial GO (> 99% purity) with sheets diameter of 2–4 μm and dispersed within 1–3 layers, and multiwalled CNTs (> 95% purity) with lengths of 0.5–2 μm and outer diameter < 8 nm were obtained from Nanjing XFNANO Materials Tech Co., Ltd, China., which was also used in our recent study (Sheng et al. 2020). According to the same manufacturer's specifications, the NG powders (> 95% purity) were characterized by layers <3, scale size of 0.5–5 μm, specific surface areas of 100–300 $m^2 \cdot g^{-1}$, and nitrogen content of ~5% wt. All the dispersions and solutions were prepared prior to use, and the deionized water (>18 MΩ·cm) was produced using Milli-Q ultrapure system (Millipore Co., USA).

Fabrication of composite membranes

According to our recent study (Sheng et al. 2020), the rGO sheets were prepared following the hydrothermal reduction protocol at 120 °C and pH 10 over 3 h, in which the GO and overheated water were employed as a precursor and reducing agent, respectively.

The fabrication of rGO/CNTs composite membrane was carried out via a pressure-driven filter method, and the filtration system comprised a peristaltic pump, a cylindrical membrane filter with filtration area of 13 cm^2 (Sartorius Co., Germany), a transmembrane pressure (TMP) sensor, Teflon tubing, feeding, and filtrate tanks, as described by Sheng et al. (2020). In short, the dispersions of rGO and CNTs were mixed in a mass ratio of 3:1 by ultrasonication (5 $W{\cdot}mL^{-1}$ of watt density) for 10 min, and then loaded onto 0.45 μm nylon support membranes (Whatman Inc., Germany) in a continuous filtration. For the NG/rGO/CNTs composite membrane, the dispersions of carbon nanomaterials were papered in an optimized mass ratio of NG:rGO:CNTs = 1.5:1.5:1, and the membrane fabrication was conducted at various carbon loading of 2–16 $g{\cdot}m^{-2}$. Thereafter, the composite membranes were sequentially washed with deionized water until the permeate being registered an ultraviolet absorbance of zero at 254 nm, and vacuum-dried at 70 °C. As described by Duan et al. (2015a), the NG shows the partially aggregated and crinkled structure. It was observed that excessive dosing NG in the membrane fabrication would deteriorate the stability of the carbon mats in aqueous solution, as evidenced by ultrasonic damage test (Fig. S1).

Operation of in situ catalytic oxidation

The in situ carbonaceous catalytic oxidation processes were carried out in the continuous and circulating filtration modes, and the carbon mats on the top of the nylon support membrane acted as the main reaction zone. In a continuous filtration experiment, 250 ml of feed solution consisting of 500 $\mu g{\cdot}L^{-1}$ SMX with various PDS dosages was passed through the composite membrane at a constant flowrate of 1.0 $mL{\cdot}min^{-1}$. The filtrate was collected at specific intervals for further analysis. For the circulating filtration mode in a loop system, the filtrate was transferred into the feeding tank under vigorous stirring at the same flowrate. The samples were periodically collected at each filtration cycle. Meanwhile, the adsorptive filtration of SMX with the composite membranes was conducted in the absence of PDS. The effects of various ROS scavengers on the SMX removal by in situ catalytic oxidation with NG/rGO/CNTs composite membrane were also investigated, in which 10 $mmol{\cdot}L^{-1}$ of methanol, sodium bicarbonate ($NaHCO_3$), and potassium iodide (KI) were added into the feed solution to scavenge $SO_4^{\cdot-}$ or/and HO·, $^1O_2$ and surface-bound $SO_4^{\cdot-}$, respectively (Chen et al. 2018).

Where required, the initial pH of solution (4, 7, and 10) was adjusted by addition of appropriate amounts of HCl or NaOH (10%), and the change of pH value was limited (±0.4) in the filtration processes. During the investigations of the effects of solution environment on the in situ catalytic oxidation, Cl^- (0–10 $mmol{\cdot}L^{-1}$), FA and TA (0–10 $mg{\cdot}L^{-1}$) were added into the feed solution under the neutral pH condition, respectively. All the filtration experiments were conducted in triplicates at a room temperature of 25 ± 2 °C.

Analytical methods

Characterization of carbon mats

Scanning electron microscopy (SEM, FEI Quanta 400, USA) was employed to characterize the morphologies of the NG/rGO/CNTs and rGO/CNTs mats. For the imaging of the cross-sections, the composite membrane was first cryo-snapped using liquid nitrogen. The thicknesses of the carbon mats were measured from the cross-sectional SEM images using a screen ruler, and their average values (δ) were calculated based on the results of multiple points. X-Ray photoelectron spectroscopy (XPS, Thermo ESCALAB 250XI, USA) was employed to probe the surface chemical components of the NG/rGO/CNTs and rGO/CNTs mats, which were freeze-dried for 12 h as a pre-treatment process. All binding energies were calibrated by the C1 peak at 284.4 eV arising from adventitious carbon. Avantage v5.52 software was used to analyze and deconvolute the obtained spectra. The surface roughness of the rGO and NG/rGO samples was evaluated using atomic force microscopy (AFM, Bruker Dimension 3100, Germany) with a scan area 10 μm × 10 μm, as operated in a tapping mode at room temperature in air. The roughness was obtained in terms of the average roughness (R_a), root-mean-square roughness R_{rms} (nm), and peak-to-valley distance (D_{max}) using NanoScope Analysis 1.8 software.

Chemicals quantitative analysis

The SMX feed and filtrate solutions were pre-treated by magnetic solid-phase extraction using carboxylated magnetic graphene oxide nanoparticles (CMGO), as described in the previous reports (Gao et al. 2018; Sheng et al. 2020). The quantification of the SMX molecule was conducted with high-performance liquid chromatography-mass spectrometry (HPLC-MS) analyses, consisting of an Ultimate 3000 HPLC system (Thermo Scientific, USA) coupled to a triple-quadrupole tandem MS (TSQ Quantum Ultra AM, USA). The separation was performed using a Zorbax Eclipse XDB-C18 reverse-phase column (50 mm × 3 mm, 1.8μm, Aglient) at 25 °C. The mobile phase consisted of a mixed solution containing methanol (A) and 0.1% formic acid (B) and the flow rate was set at 0.2 $mL{\cdot}min^{-1}$. The retention time and

mass-to-charge ratio (m/z) of the SMX were 4.8 min and 253.9, respectively, and the detection limit for this method was in the range of 10–20 ng·L^{-1}.

The quantification of FA and TA contents in aqueous solution was conducted on the basis of the linear relation between their mass concentrations and ultraviolet absorbance on the fixed wavelengths (254 nm for FA, 275 nm for TA) using UV-visible spectrophotometer (Persee T700, China). The concentrations of ammonia nitrogen (NH_4^+-N), total nitrogen (TN), and mixed liquor volatile suspended solid (MLVSS) were determined using the procedure described in Standard Methods (American Public Health Association 1998).

The microbial inhibition assessment of oxidation intermediates

To assess the ecotoxicity potential of parent SMX and intermediate products with the in situ catalytic oxidation, the partial nitritation and anaerobic ammonium oxidation (PN/A) granular sludge showing a higher sensitivity to toxic compounds than conventional activated sludge was employed for testing the specific nitrogen removal rate (q value) in various solution environments with initial NH_4^+-N concentration of 100 mg·L^{-1} (Qian et al. 2017).

Prior to the q testing of PN/A granules, the aqueous solutions (100 ml) of oxidation intermediates without inorganic salts were prepared using solid-phase extraction workstation with HLB cartridge (WAT106202, Waters Oasis®, USA) following the modified procedure described by Ji et al. (2015). Then, the q_{test} values of granules were obtained with batch activity tests exposed to SMX and oxidation intermediate solutions with various dilution ratios, while the aqueous solution without SMX was used as blank group for q_0 value. The average q_0 values of granules as NH_4^+-N and TN were estimated at 27.8 mg·$gVSS^{-1}$·h^{-1} and 23.4 mg·$gVSS^{-1}$·h^{-1} respectively, and the inhibition effects of solution environments on the microbial activity were evaluated as 1-q_{test}/q_0 (%).

Calculations

The pure water flux as J_w (L·(m^2·h·bar)$^{-1}$) of the composite membrane was measured at constant pressure of 0.9 bar and calculated as follows:

$$J_w = V/(A \times \Delta p \times t) \quad (1)$$

where t is the filtration time, h; V is the permeate volume during t, L; A is the effective filtration area, 13×10^{-4} m^2; and Δp is the TMP, bar.

The filtration behaviors of pure water can be described by the generic Carman equation for constant pressure dead-end filtration. The filtration resistance of the composite membrane as R_m (m^{-1}) and the specific filtration resistance of the carbon mats as r_c (m^{-2}) were calculated as follows, respectively (Huang et al. 2018):

$$R_m = 1/(J_w \times \mu) \quad (2)$$

$$r_c = (R_m - R_{m0})/\delta \quad (3)$$

where μ is the water viscosity at 25 °C, 8.937×10^{-4} Pa·s; R_{m0} is the filtration resistance of nylon support membrane, 3.0×10^{10} m^{-1}; and δ is the mean thickness of the carbon mats, m.

For the in situ carbonaceous catalytic oxidation, the contact time (t_c, s) of the feed solution in the carbon mats was calculated as follows:

$$t_c = (60 \times \delta \times A)/q \quad (4)$$

where q is the constant flowrate of membrane filtration, 1×10^{-6} m^3·min^{-1}.

The SMX removal rate as r_{SMX} (mg·m^{-2}·h^{-1}) of in situ carbonaceous catalytic oxidation under the continuous filtration mode was obtained as follows (Vieira et al. 2020):

$$r_{SMX} = 60 \times 1000 \times q \times (c_{inf} - c_{eff})/A \quad (5)$$

where c_{inf} and c_{eff} are the SMX concentrations in the feed and filtrate solution, respectively, mg·L^{-1}.

The specific nitrogen removal rate of PN/A granules was determined using the following equation (Bassin et al. 2012):

$$q_{test} = -\Delta c/(\Delta t \cdot \mathrm{VSS}) \quad (6)$$

where Δc is the differences in concentrations of NH_4^+-N or TN during Δt, mg·L^{-1}; Δt is the time period of batch tests corresponding to the linear variation of concentration of nitrogen compounds, in h; and VSS is the MLVSS concentration of granular sludge, in g·L^{-1}.

Results and discussion

Characterization of the composite carbon mats

Figure 1 shows the surface morphology and cross-section of the composite carbon mats observed using SEM. During the filtration assembly, graphene sheets were crosslinked with each other in a parallel manner forming typical laminar structures for molecules separation, while the well-dispersed CNTs were intercalated into the stacked graphene-based layers, creating capillary nanochannels for water delivery (Gao et al. 2015). AFM images (Fig. S2) demonstrate that the addition of NG significantly increased the surface roughness of the composite rGO structures. Observations of the NG/rGO/CNTs mats exhibited a looser stacking morphology (2.2-fold larger δ value in Table 1) than rGO/CNTs mats at the same carbon loading, which revealed a larger width of water

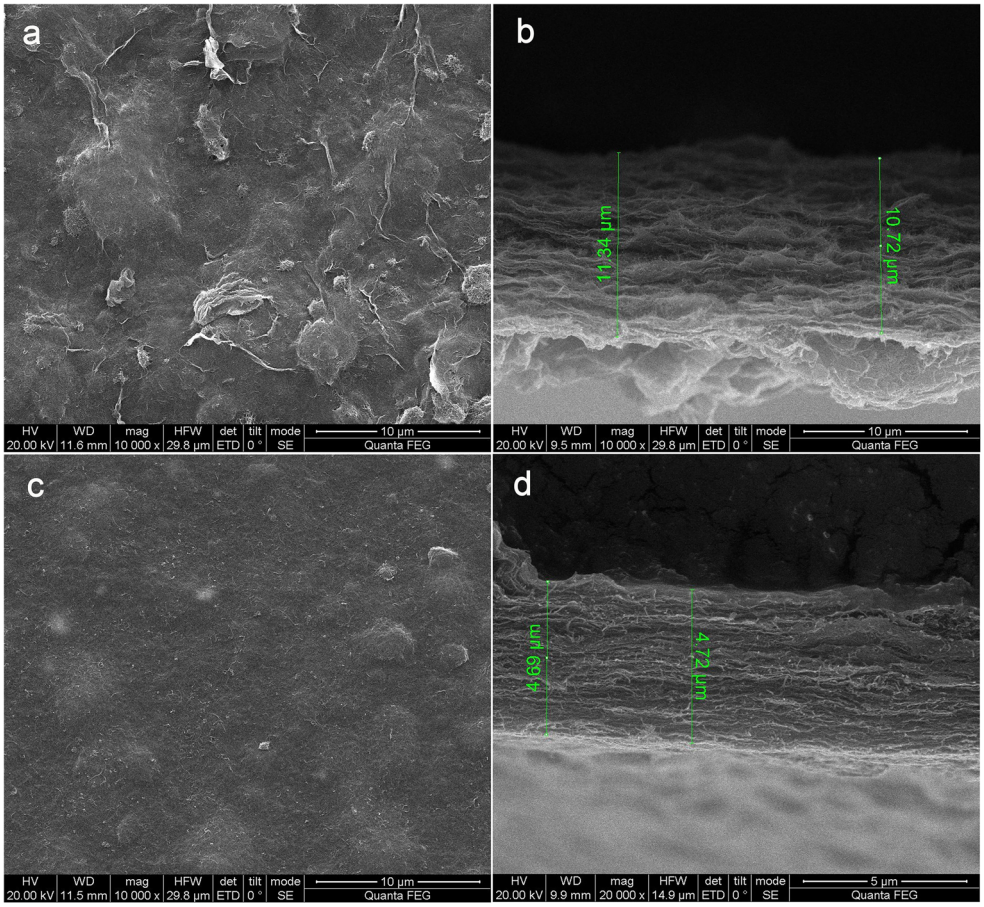

Fig. 1 Top-view and cross-sectional SEM images of NG/rGO/CNTs (**a**, **b**) and rGO/CNTs (**c**, **d**) mats at a carbon loading of 8 g·m^{-2}

delivery channels with low mass-transfer resistance was obtained in the former.

Table 1 gives the surface chemical components based on XPS analysis and water permeability performance using dead-end filtration in the composite membranes. It was worth noting that an atomic ratio of carbon to oxygen (C/O ratio) of 3.89 indicated that the NG/rGO/CNTs mats had hydrophobic interfaces with fewer oxygen-containing functional groups than rGO/CNTs (C/O = 2.91) (Sheng et al. 2020), where there was a significant difference in the N species found in the two types of carbon mats (Table S1). As a result, the NG/rGO/CNTs composite membranes showed a higher J_w with a low r_c value, such that a superior low-pressure filtration performance could be expected to operate the in situ catalytic oxidation.

In situ catalytic oxidation with composite membranes

As shown in Fig. 2a, the removal efficiency of SMX by adsorptive filtration decreased strictly within 60 min under the continuous filtration mode, but the NG/rGO/CNTs composite membrane had notable advantages with respect to the adsorption affinity for SMX molecules through intraparticle diffusion, hydrophobic effects, and π-π interactions during tortuous flow in carbon mats (Wang et al. 2017), as the former had a 2-fold higher SMX removal than the rGO/CNTs mats in circulating filtration over 3 cycles (Fig. 2b). The similar result was also reported by Song et al. (2021), where the adsorption capacity of N-doped rGO for polycylic aromatic hydrocarbons (PAHs) was 1.4-fold larger than that of rGO in a batch test at pH 7.

Table 1 Characterization of the NG/rGO/CNTs and rGO/CNTs mats

Carbon nanomaterial	Mats structure				Filtration performance		
	δ (μm)	C (at%)	O (at%)	N (at%)	J_w (L· m^{-2}·h^{-1}·bar^{-1})	R_m (×10^{12} m^{-1})	r_c (×10^{18} m^{-2})
NG/rGO/CNTs	10.5 ± 0.4	77.07	19.83	3.10	93.62	4.35	0.41
rGO/CNTs	4.7 ± 0.2	71.91	24.71	3.38	38.34	10.61	2.26

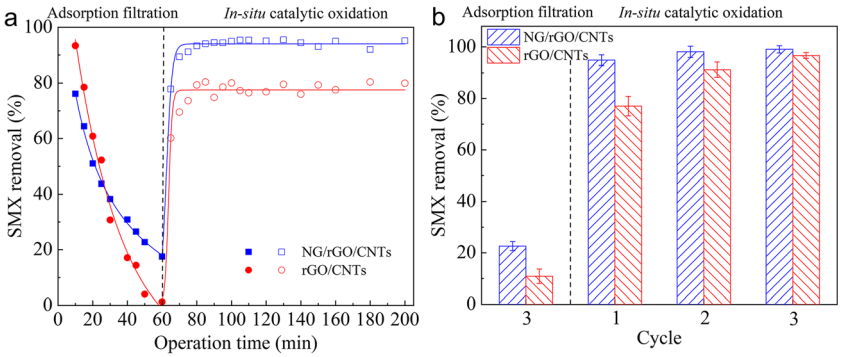

Fig. 2 Comparison of SMX removal by the adsorptive filtration and in situ catalytic oxidation with the rGO/CNTs and NG/rGO/CNTs composite membranes under the **a** continuous and **b** circulating filtration modes (carbon loading of 8 g·m^{-2}, PDS dosage of 5 mmol·L^{-1})

Previous studies have reported that the abatement of SMX by PDS oxidation was negligible in the absence of carbonaceous catalysts (Guan et al. 2019; Sheng et al. 2020), but dosing PDS of 5 mmol·L^{-1} to drive the in situ catalytic oxidation processes significantly improved the removal of SMX. The removal efficiency of SMX on 94.3 ± 1.3 % in a short t_c of 0.82 s was obtained with the NG/rGO/CNTs composite membrane, corresponding to a SMX removal rate (r_{SMX}) of 21.7 ± 0.3 mg·m^{-2}·h^{-1}, which exceed that of the rGO/CNTs by approximately 17% over 140 min of continuous filtration (Sheng et al. 2020). In addition, the NG/rGO/CNTs composite membrane with single circulating filtration provided a comparable SMX removal by activating PDS during the 3-cycle filtration of the rGO/CNTs (Fig. 2b).

Based on these results, the effects of carbon loading and PDS dosage on the SMX removal and operation of the TMP in the in situ catalytic oxidation of the NG/rGO/CNTs composite membrane were investigated in more detail. Fig. S3 and Fig. S4 demonstrate that a carbon loading of 8 g·m^{-2} was the ideal dosage to achieve efficient and stable SMX removal with a low TMP, when adequate PDS (≥2 mmol·L^{-1}) was used as the ROS precursor in the in situ catalytic oxidation. Compared with the rGO/CNTs composite membrane, the superior performance of the NG/rGO/CNTs can be described by a high SMX removal efficiency over 90% with a relatively lower PDS dosage (2 mmol·L^{-1}) and energy savings (TMP 0.6 bar) for filtration operation at the same carbon loading, as illustrated in Fig. 3.

Table S1 lists the atomic percentages of C1, O1, and N1 in the NG/rGO/CNTs and rGO/CNTs mats obtained by XPS analysis. In accordance with the differentiated removal efficiencies of SMX, the NG/rGO/CNTs mats contained a higher contents of sp^2 hybridized C and carbonyl group (C=O) as typical Lewis basic sites than the rGO/CNTs mats, as well as being enriched in active N-doped species for PDS activation (Frank et al. 2009; Pan et al. 2018), including pyridinic N in a 6-membered ring on the graphene defects and graphitic N doped in conjugated carbon network. These results provide evidence for the involvement of both radical and non-radical pathways in the in situ catalytic oxidation for SMX degradation, which can be proved by the influences of various ROS scavengers (Fig. S5). As graphitic N doping can not only contribute active the sp^2 hybridized carbon lattice by creating free-flowing π-electrons, as well as producing high oxidative radicals via electron transfer to persulfates (Ren et al. 2020; Sun et al. 2013), but also yield positively charged of adjacent carbon atoms, facilitating the formation of surface-activated persulfate via electrostatic bonding for the non-radical pathway (Li et al. 2017).

As shown in Fig. 4 and listed in Table 2, the XPS spectra of the NG/rGO/CNTs mats that experienced in situ catalytic oxidation also confirms that the carbon framework and defects were partially oxidized by ROS (Liu et al. 2016; Pan et al. 2018), with the production of oxygen-containing functional groups (such as C-O-C and C=O) and reduction in the C/O ratio of the carbon mats (2.96 after PDS activation). Graphitic

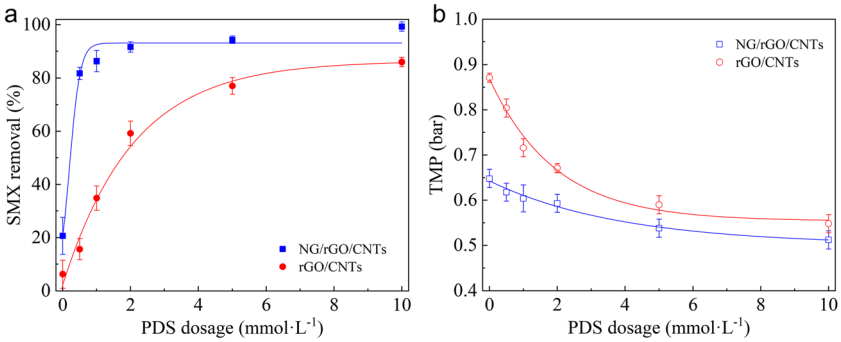

Fig. 3 Effects of PDS dosage on the **a** SMX removal and **b** operation TMP of the in situ carbonaceous catalytic oxidation processes under the circulating filtration mode

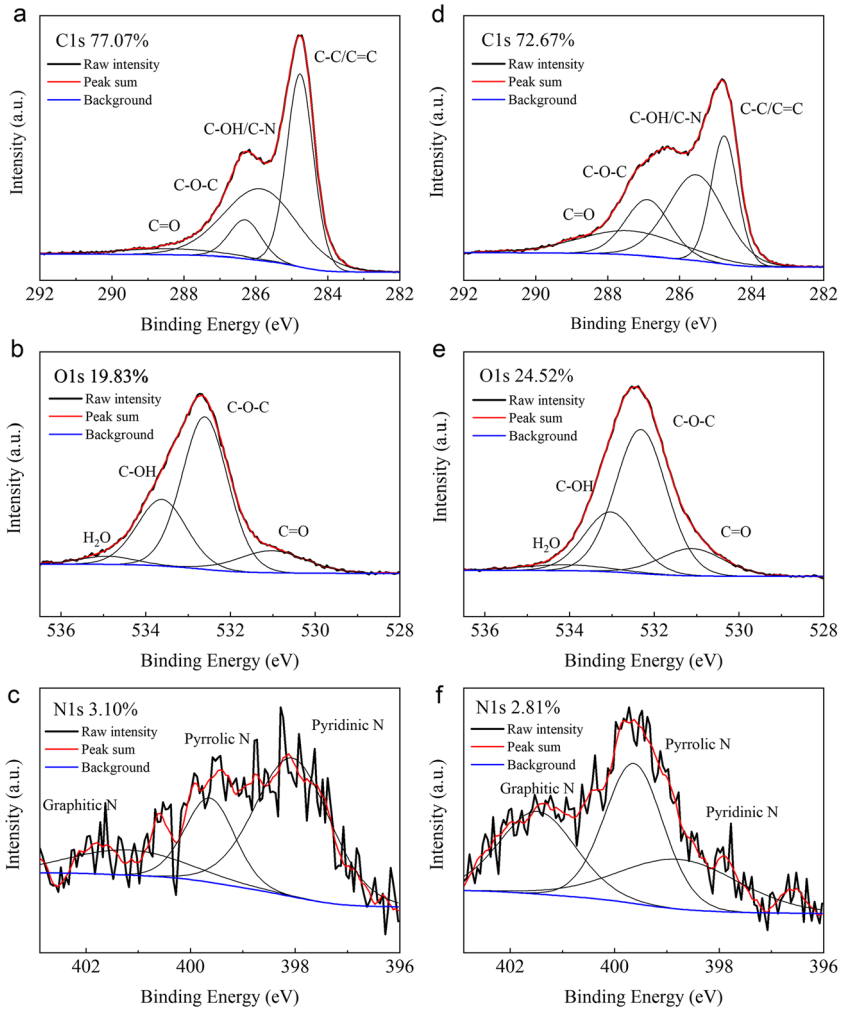

Fig. 4 The high-resolution C1s, O1s, and N1s patterns in XPS spectra of the NG/rGO/CNTs mats **a**–**c** before and **d**–**f** after in situ catalytic oxidation treatment

N exhibited a stronger oxidation resistance than pyridinic N as Lewis basic sites (reduced by 45 at%). This result was in agreement with Pedrosa et al. (2019), who observed that graphitic N can contribute to maintaining some of the catalytic activity of N-doped rGO in terms of its reusability assessment for persulfate activation. Owing to the complex compositions of the NG/rGO/CNTs mats, further mechanistic details concerning the contribution of various active sites for ROS producing in the system remain to be ascertained.

Table 2 Distribution of the Cls, O1s, and N1s bonds in the NG/rGO/CNTs mats before and after in situ catalytic oxidation treatment

Atomic species	Location (eV)	Group	Atomic percentage (%)	
			Before	After
C1s	284.4	C-C/C=C	59.68	25.51
	285.8	C-OH/C-N	32.95	36.66
	286.7	C–O-C	3.69	19.12
	288.0	C=O	3.68	18.71
O1s	530.7	C=O	59.55	60.44
	531.8	C-O-C	12.61	13.99
	533.1	C-OH	27.84	25.57
N1s	398.4	Pyridinic N	47.62	29.02
	399.6	Pyrrolic N	26.73	40.09
	401.1	Graphitic N	25.65	30.89

Previous studies have reported that the transformation mechanisms of SMX by ROS mainly involve electrophilic attack on the aniline moiety, hydroxylation of the aniline moiety and isoxazole ring, cleavage of the sulfonamide S–N bond, and coupling process (Ji et al. 2015; Yang et al. 2017). Figure 5 illustrates that the in situ catalytic oxidation of the NG/rGO/CNTs composite membrane is a good alternative for SMX degradation with detoxifying intermediate products, as the inhibition effects ($1\text{-}q_{test}/q_0$) of its filtrate on the specific nitrogen removal activities of PN/A granular sludge were lower than the feed solution of SMX. With an efficient SMX removal through in situ catalytic oxidation, the NG/rGO/CNTs composite membrane showed a relatively stronger detoxification ability, as q_{test}/q_0 was larger at all dilution ratios

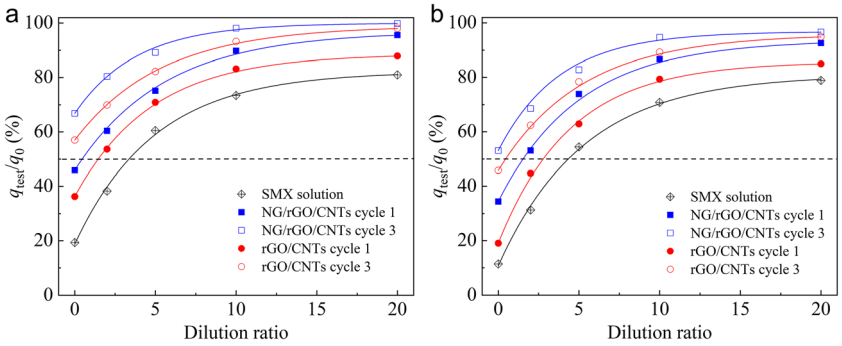

Fig. 5 The SMX detoxification assessment of in situ carbonaceous catalytic oxidation processes (carbon loading of 8 $g \cdot m^{-2}$, PDS dosage of 5 $mmol \cdot L^{-1}$) using the specific nitrogen removal activities of granules (as a: NH_4^+-N; b: TN)

from 0 to 20-fold, than that of the rGO/CNTs, which can be enhanced with an increase in the number of circulating filtration.

A similar observation was also reported by Guan et al. (2019), where the mineralization of SMX was highly limited during PDS activation by CNTs, and the hydroxylated and isoxazole ring opening products showed generally lower ecotoxicity value as compared with the parent SMX using ECOSAR program. Given the notable positive correlation between the metabolites of SMX and its octanol-water partition coefficients (K_w), the incremental hydrophilicity of oxidative products may result in a decrease in their toxicity (Lienert et al. 2007).

Influences of solution environment

The influences of solution pH

As displayed in Fig. 6, the solution pH significantly affects the SMX removal and TMP of the in situ carbonaceous catalytic oxidation during membrane filtration at a fixed PDS dosage and carbon loading. For the two types of composite membranes, the SMX removal observed at pH 7 was appreciably higher than those observed at pH 4 and pH 10 during circulating filtration, while the lowest TMP was obtained at neutral pH condition. However, the initial pH, which was adjusted to be more acidic or alkaline, showed weaker inhibitions for the performance of NG/rGO/CNTs composite membrane, as compared with that of the rGO/CNTs, which should be closely related to the differentiation of the reaction mechanisms in systems.

It is well known that dissociated SMX ions ($pK_{a1} = 1.83$, $pK_{a2} = 5.57$) have higher electron densities and are thus more susceptible to ROS oxidation than nondissociated ones (Guan et al. 2019), while both SMX and PDS molecules show stronger affinities for graphene-based surface via electrostatic interactions under acidic conditions, which is favorable for the electron transfer in redox reactions (Ren et al. 2020; Wang et al. 2017).

In this study, a significant pH enhancement in the hydrolysis of PDS to generate reactive radical species could not be involved in the in situ catalytic oxidation, since strongly acid

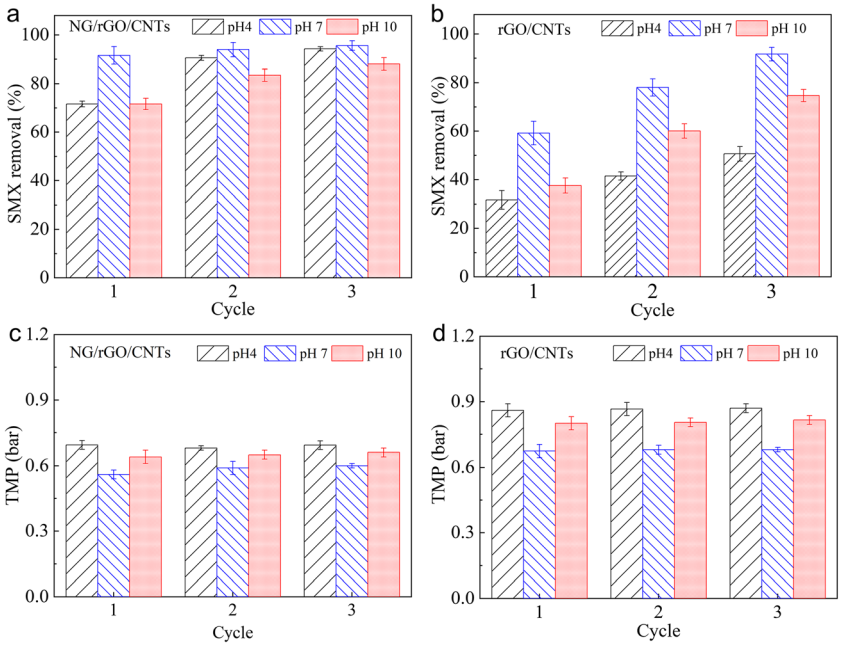

Fig. 6 Effects of the solution pH on the **a**, **b** SMX removal and **c**, **d** operation TMP of in situ carbonaceous catalytic oxidation processes under the circulating filtration mode (carbon loading of 8 $g \cdot m^{-2}$, PDS dosage of 2 $mmol \cdot L^{-1}$)

(pH < 2) and alkaline (pH > 11) conditions were not employed (Ahmad et al. 2013). According to Duan et al. (2015b), changes in the solution pH had a negligible effect on PDS activation triggered by pyridinic N on the graphene defects and sp^2 carbon adjacent to graphitic N. For the NG/rGO/CNTs composite membrane, a balance between radical and non-radical pathways in the oxidation systems may be achieved at pH 7.0, which also results in a low TMP for filtration operation by affecting electronic characteristics of the carbon mats.

The influences of Cl^- concentration

Given that chlorine ions that exist extensively in real waterbody can act as radical scavenger, experiments on the influences of Cl^- concentration on in situ carbonaceous catalytic oxidation were conducted at neutral pH. As shown in Fig. 7, the addition of 4 mmol·L^{-1} Cl^- reduced the removal efficiency of SMX by 20% for the NG/rGO/CNTs composite membrane and 30% for the rGO/CNTs one after 1 cycle of circulating filtration, while the increase in the TMP of the latter was approximately 2-fold larger than that of the former. The adverse effects of Cl^- can be due to the oxidation of Cl^- by free radicals to Cl·, which rapidly combines with another chloride to form $Cl_2^{\cdot-}$ (chlorine radical, $E^0_{Cl2\cdot-/2Cl} = 2.09$ V), characterized by a lower oxidation potential than $SO_4^{\cdot-}$ and HO· (Chen and Carroll 2016; Zhang et al. 2014). In addition, the relatively stronger resistance of the NG/rGO/CNTs composite membrane to Cl^- exposure indicated that the non-radical pathway plays an important role in in situ catalytic oxidation for SMX degradation. Because the moderate non-radical complexes were unable to effectively oxidize the halogen ions (Guan et al. 2017).

However, when the Cl^- concentration continued to increase to 10 mmol·L^{-1}, a distinct improvement in the organic degradation and operation TMP of in situ catalytic oxidation was observed. In particular, both the SMX removal and operation TMP of the NG/rGO/CNTs composite membrane reached comparable levels in the absence of Cl^-. A similar phenomenon was also reported in the PDS activation by mesoporous carbon for the degradation of 2,4-dichlorophenol (Tang et al. 2018). This result can be reasonably interpreted by the fact that the superabundant negative charge of Cl^- can serve as an electron donor to donate electrons to PDS, resulting in the generation of excess ROS in in situ catalytic oxidation. The relationship between the ROS species and ion strength should be investigated in future studies.

The influences of background organics

FA, a typical aromatic substance with small molecules, is ubiquitous in aqueous environments. As shown in Fig. 8a and Fig. S6, the presence of FA substantially suppressed the removal of SMX in both adsorptive filtration and in situ catalytic oxidation. As the FA concentration increased from 0 to 10 mg·L^{-1}, the removal efficiencies of SMX with the NG/rGO/CNTs and rGO/CNTs composite membranes after 3 cycles of circulating filtration were reduced by 33.8 % and 56.4 %, respectively (Fig. 8a), while a dramatic increase in the FA removal was observed (Fig. 8b). The negative effects of FA can be reasonably explained by their redox property as an electron acceptor, where FA at high concentrations

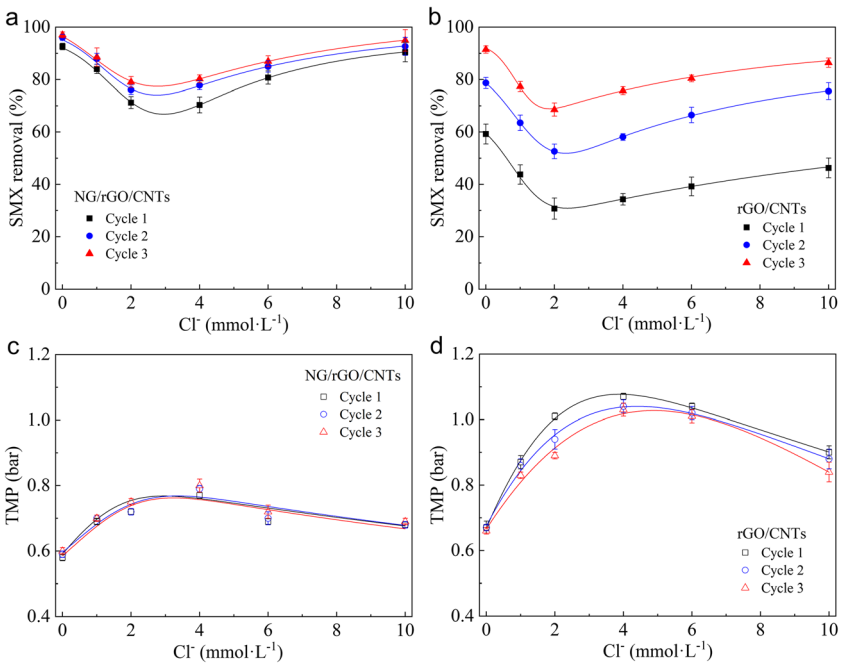

Fig. 7 Effects of Cl^- concentration on the **a**, **b** SMX removal and **c**, **d** operation TMP of in situ catalytic carbonaceous oxidation processes under the circulating filtration mode (carbon loading of 8 g·m^{-2}, PDS dosage of 2 mmol·L^{-1}, solution pH 7)

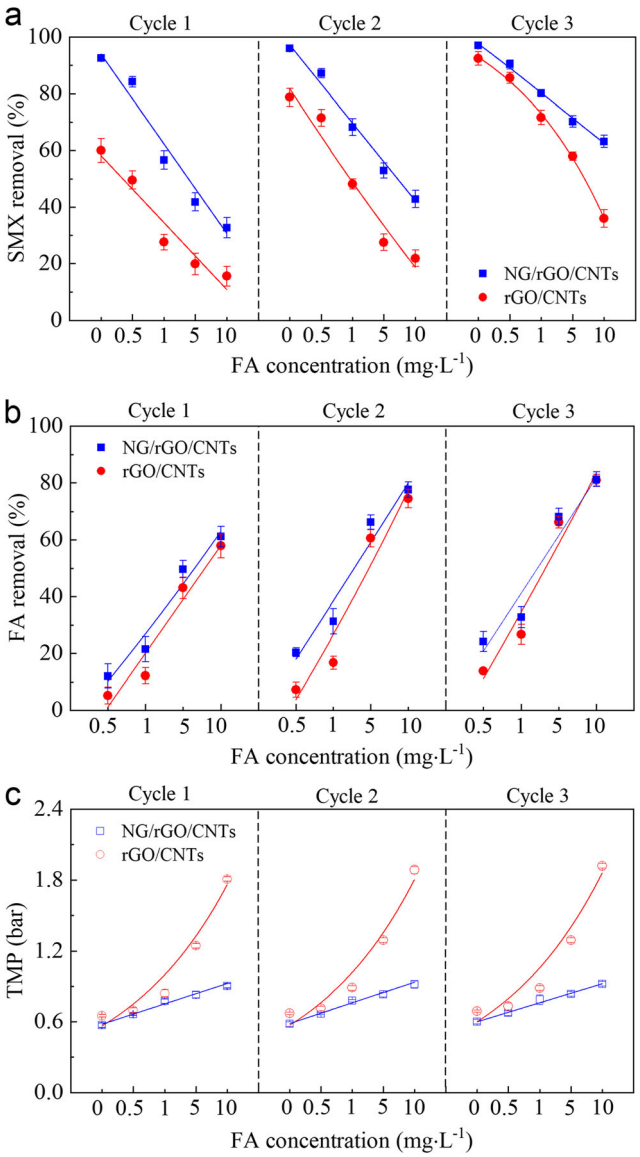

Fig. 8 Effects of FA concentration on the **a** SMX removal, **b** FA removal, and **c** operation TMP of in situ carbonaceous catalytic oxidation processes under the circulating filtration mode (carbon loading of 8 g·m^{-2}, PDS dosage of 2 mmol·L^{-1}, solution pH 7)

competitively consumed the ROS from PDS activation and interfered with the electron transfer from SMX to PDS (Chen and Carroll 2016; Gao et al. 2020). Furthermore, some surface active sites in the carbon mats were inevitably obstructed by the accumulation of oxidation intermediates on the membrane, thus causing an increase in the operation TMP at high FA concentrations. Based on the aforementioned results, the loose laminar structure of the NG/rGO/CNTs mats appears to be favorable for resisting membrane fouling, based on TMP variations with increasing FA concentration (Fig. 8c).

In contrast, TA at low concentration (0.5 mg·L^{-1}) has a negligible influence on SMX degradation via in situ catalytic oxidation of the NG/rGO/CNTs composite membrane, and a sharp decline was observed with increasing TA concentration in the solution (Fig. 9a and Fig. S7). When the FA concentration was as high as 10 mg·L^{-1}, only 13.2 ± 1.9 % and 9.2 ± 1.0 % SMX were removed after 3 cycles of circulating filtration with the NG/rGO/CNTs and rGO/CNTs composite membranes, respectively, revealing the stronger inhibition effects of TA at high concentrations, as compared with FA.

Given that TA has a 5.7-fold larger molecular weight with abundant oxygen-containing functional groups (carboxyl and phenolic groups) than that of SMX, TA prefers to influences the adsorption and oxidation of SMX by acting as a competitor or modifying the surface properties of the carbon mats. According to Wang et al. (2017), carboxylic and hydorxyl groups in NOM can weaken the complexation between

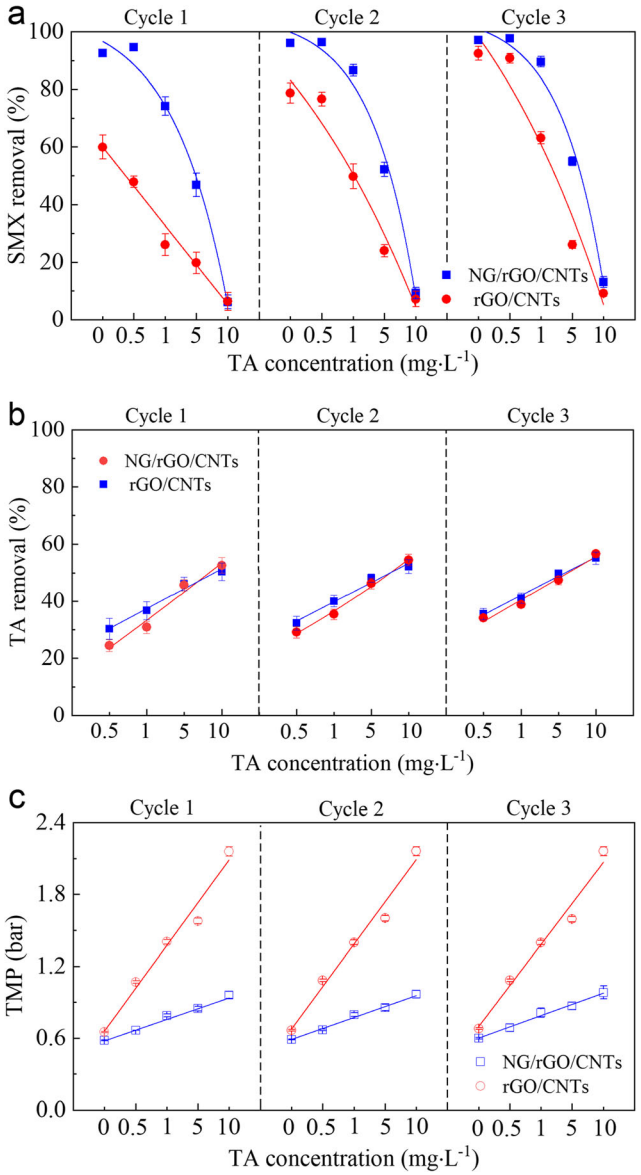

Fig. 9 Effects of TA concentration on the **a** SMX removal, **b** TA removal, and **c** operation TMP of in situ carbonaceous catalytic oxidation processes under the circulating filtration mode (carbon loading of 8 g·m^{-2}, PDS dosage of 2 mmol·L^{-1}, solution pH 7)

SMX and the graphitic surface via electrostatic repulsion and steric hindrance. Electron-rich TA at high concentrations has a notable advantage over SMX and PDS in competing for the surface active sites of the carbon mats, and the decline in the free radicals and non-radical reactive complexes formation were responsible for the decrease in SMX removal. As shown in Fig. 9b and c, the accumulation of TA and oxidation intermediates on the membrane was confirmed by the nearly linear increase in the operation TMP with varying TA concentrations. Similar NOM-induced inhibition was also observed during the oxidation of phenol compounds via carbonaceous catalytic oxidation (Duan et al. 2015a; Guan et al. 2017; Tang et al. 2018).

Conclusions

In summary, NG/rGO/CNTs composite membrane is effective for the degradation of SMX by activating PDS to operate the in situ catalytic oxidation process, achieving a r_{SMX} of 21.7 $mg \cdot m^{-2} \cdot h^{-1}$ under the continuous filtration mode. Compared with the rGO/CNTs mats in our previous study, the NG/rGO/CNTs mats exhibited a looser laminar structure with a stronger hydrophobic surface, in which pyridinic and graphitic N were proposed to play important roles in enhancing their catalytic activity. Moreover, solution environment, including the solution pH, Cl^-, and background organics, had notable influences on the performance of in situ catalytic oxidation with composite membranes, indicating that both radical and non-radical pathways were involved in systems. Alternatively, the NG/rGO/CNTs composite membrane is a promising metal-free persulfates catalyst for organic pollutant oxidation in real water purification, and further studies are required to enhance the reaction selectivity and stability for the long-term operation.

Supplementary Information The online version contains supplementary material available at https://doi.org/10.1007/s11356-021-12545-1.

Acknowledgments The authors acknowledge the support from the Qinglan Project for Jiangsu Colleges and Universities, China.

Authors' contributions Feiyue Qian developed the research proposal, and was a major contributor in writing the manuscript; Honggui Yin and Jiayi Sheng performed the fabrication of composite membranes and in situ catalytic oxidation for SMX degradation, analyzed the original experiment data; Shiqian Gao developed the quantitative analysis methods of SMX at low concentration, and was responsible for the extraction of oxidation intermediates from the filtrate. Feng Liu designed the system of in situ catalytic oxidation, and interpreted the results regarding the effects of solution environment; Yaoliang Shen gave important suggestions in the improvement of this manuscript. All authors read and approved the final manuscript.

Funding This study was supported by the National Natural Science Foundation of China (51608341), the Natural Science Foundation of Jiangsu Province, China (BK20150284), and the Open Project of National & Local Joint Engineering Laboratory for Municipal Sewage Resource Utilization Technology (No.2019KF02).

Data availability All data generated or analyzed during this study are included in this published article (and its supplementary information files).

Compliance with ethical standards

Ethics approval and consent to participate Not applicable.

Consent for publication Not applicable.

Competing interests The authors declare no competing interests.

References

Ahmad M, Teel AL, Watts RJ (2013) Mechanism of persulfate activation by phenols. Environ Sci Technol 47(11):5864–5871

American Public Health Association (1998) Standard methods for examination of water and wastewater, 20th edn. American Water Works Association, Washington DC

Bassin JP, Kleerebezem R, Dezotti M, van Loosdrecht MC (2012) Measuring biomass specific ammonium, nitrite and phosphate uptake rates in aerobic granular sludge. Chemosphere 89(10):1161–1168

Chen H, Carroll KC (2016) Metal-free catalysis of persulfate activation and organic-pollutant degradation by nitrogen-doped graphene and aminated graphene. Environ Pollut 215:96–102

Chen X, Oh WD, Lim TT (2018) Graphene- and CNTs-based carbocatalysts in persulfates activation: material design and catalytic mechanisms. Chem Eng J 354:941–976

Cheng X, Guo H, Zhang Y, Korshin GV, Yang B (2019) Insights into the mechanism of nonradical reactions of persulfate activated by carbon nanotubes: activation performance and structure-function relationship. Water Res 157:406–414

Devi P, Das U, Dalai AK (2016) In-situ chemical oxidation: principle and applications of peroxide and persulfate treatments in wastewater systems. Sci Total Environ 571:643–657

Duan X, Ao Z, Sun H, Indrawirawan S, Wang Y, Kang J, Wang S (2015a) Nitrogen-doped graphene for generation and evolution of reactive radicals by metal-free catalysis. ACS Appl Mater Interfaces 7(7):4169–4178

Duan X, O'Donnell K, Sun H, Wang Y, Wang S (2015b) Sulfur and nitrogen Co-doped graphene for metal-free catalytic oxidation reactions. Small 11(25):3036–3044

Fang G, Gao J, Dionysiou DD, Liu C, Zhou D (2013) Activation of persulfate by quinones: free radical reactions and implication for the degradation of PCBs. Environ Sci Technol 47(9):4605–4611

Frank B, Zhang J, Blume R, Schlogl R, Su DS (2009) Heteroatoms increase the selectivity in oxidative dehydrogenation reactions on nanocarbons. Angew Chem Int Ed Eng 48(37):6913–6917

Gao SJ, Qin H, Liu P, Jin J (2015) SWCNT-intercalated GO ultrathin films for ultrafast separation of molecules. J Chromatogr A 3(12):6649–6654

Gao PS, Guo Y, Li X, Wang X, Wang J, Qian F, Zhang Z (2018) Magnetic solid phase extraction of sulfonamides based on carboxylated magnetic graphene oxide nanoparticles in environmental waters. J Chromatogr A 1575:1–10

Gao J, Luo C, Gan L, Wu D, Tan F, Cheng X, Zhou W (2020) A comparative study of UV/H_2O_2 and UV/PDS for the degradation of

micro-pollutants: kinetics and effect of water matrices. Environ Sci Pollut Res 27(19):24531–24541

Guan C, Jiang J, Pang S, Luo C, Ma J, Zhou Y, Yang Y (2017) Oxidation kinetics of bromophenols by nonradical activation of peroxydisulfate in the presence of carbon nanotube and formation of brominated polymeric products. Environ Sci Technol 51(18): 10718–10728

Guan C, Jiang J, Pang S, Ma J, Chen X, Lim TT (2019) Nonradical transformation of sulfamethoxazole by carbon nanotube activated peroxydisulfate: kinetics, mechanism and product toxicity. Chem Eng J 378(15):122147

Huang H, Sheng J, Qian F, Zhou F, Gao S, Shen X (2018) Effects of graphene oxide incorporation on the mat structure and performance of carbon nanotube composite membranes. Res Chem Intermed 45: 533–548

Isidori M, Lavorgna M, Nardelli A, Pascarella L, Parrella A (2005) Toxic and genotoxic evaluation of six antibiotics on non-target organisms. Sci Total Environ 346(13):87–98

Ji Y, Fan Y, Liu K, Kong D, Lu J (2015) Thermo activated persulfate oxidation of antibiotic sulfamethoxazole and structurally related compounds. Water Res 87:1–9

Lei Y, Chen CS, Tu YJ, Huang YH, Zhang H (2015) Heterogeneous degradation of organic pollutants by persulfate activated by CuO-Fe_3O_4: mechanism, stability, and effects of pH and bicarbonate ions. Environ Sci Technol 49(11):6838–6845

Li D, Duan X, Sun H, Kang J, Zhang H, Tade MO, Wang S (2017) Facile synthesis of nitrogen-doped graphene via low-temperature pyrolysis: the effects of precursors and annealing ambience on metal-free catalytic oxidation. Carbon 115:649–658

Lienert J, Gudel K, Escher BI (2007) Screening method for ecotoxicological hazard assessment of 42 pharmaceuticals considering human metabolism and excretory routes. Environ Sci Technol 41(12): 4471–4478

Liu Y, Yu L, Ong CN, Xie J (2016) Nitrogen-doped graphene nanosheets as reactive water purification membranes. Nano Res 9:1983–1993

Liu H, Liu Y, Tang L, Wang J, Xie Q (2020) Egg shell biochar-based green catalysts for the removal of organic pollutants by activating persulfate. Sci Total Environ 745:141095

Matta R, Tlili S, Chiron S, Barbati S (2010) Removal of carbamazepine from urban wastewater by sulfate radical oxidation. Environ Chem Lett 9(3):347–353

Pan X, Chen J, Wu N, Qi Y, Xu X, Ge J, Wang X (2018) Degradation of aqueous 2,4,4′-Trihydroxybenzophenone by persulfate activated with nitrogen doped carbonaceous materials and the formation of dimer products. Water Res 143:176–187

Pedrosa M, Drazic G, Tavares PB, Figueiredo JL, Silva AMT (2019) Metal-free graphene-based catalytic membrane for degradation of organic contaminants by persulfate activation. Chem Eng J 369: 223–232

Qi C, Liu X, Ma J, Lin C, Li X, Zhang H (2016) Activation of peroxymonosulfate by base: implications for the degradation of organic pollutants. Chemosphere 151:280–288

Qian F, Chen X, Wang J, Shen Y, Gao J, Mei J (2017) Differentiation in nitrogen-converting activity and microbial community structure between granular size fractions in a continuous autotrophic nitrogen removal reactor. J Microbiol Biotechnol 27(10):1798–1807

Ren W, Nie G, Zhou P, Zhang H, Duan X, Wang S (2020) The intrinsic nature of persulfate activation and N-doping in carbocatalysis. Environ Sci Technol 54(10):6438–6447

Sheng J, Yin H, Qian F, Huang H, Gao S, Wang J (2020) Reduced graphene oxide-based composite membranes for in-situ catalytic oxidation of sulfamethoxazole operated in membrane filtration. Sep Purif Technol 236:116275

Song T, Tian W, Qiao K, Zhao J, Chu M, Du Z, Wang L, Xie W (2021) Adsorption behaviors of polycyclic aromatic hydrocarbons and oxygen derivatives in wastewater on N-doped reduced graphene oxide. Sep Purif Technol 254:117565

Sun H, Wang Y, Liu S, Ge L, Wang L, Zhu Z, Wang S (2013) Facile synthesis of nitrogen doped reduced graphene oxide as a superior metal-free catalyst for oxidation. Chem Commun 49(85):9914–9916

Tang L, Liu Y, Wang J, Zeng G, Deng Y, Dong H, Peng B (2018) Enhanced activation process of persulfate by mesoporous carbon for degradation of aqueous organic pollutants: electron transfer mechanism. Appl Catal B Environ 231:1–10

Vieira O, Ribeiro RS, Pedrosa M, Lado Ribeiro AR, Silva AMT (2020) Nitrogen-doped reduced graphene oxide – PVDF nanocomposite membrane for persulfate activation and degradation of water organic micropollutants. Chem Eng J 402:126117

Wang F, Ma S, Si Y, Dong L, Wang X, Yao J, Xing B (2017) Interaction mechanisms of antibiotic sulfamethoxazole with various graphene-based materials and multiwall carbon nanotubes and the effect of humic acid in water. Carbon 114:671–678

Yang Y, Lu X, Jiang J, Ma J, Liu G, Cao Y, Luo C (2017) Degradation of sulfamethoxazole by UV, UV/H_2O_2 and UV/persulfate (PDS): formation of oxidation products and effect of bicarbonate. Water Res 118:196–207

Yu J, Feng H, Tang L, Pang Y, Zeng G, Lu Y, Wang J (2020a) Metal-free carbon materials for persulfate-based advanced oxidation process: microstructure, property and tailoring. Prog Mater Sci 111:100654

Yu J, Tang L, Pang Y, Zeng G, Feng H, Zou J, Tan J (2020b) Hierarchical porous biochar from shrimp shell for persulfate activation: a two-electron transfer path and key impact factors. Appl Catal B-Environ 260:118160

Zhang T, Chen Y, Wang Y, Le Roux J, Yang Y, Croue JP (2014) Efficient peroxydisulfate activation process not relying on sulfate radical generation for water pollutant degradation. Environ Sci Technol 48(10):5868–5875

Zhang M, Chen X, Zhou H, Murugananthan M, Zhang Y (2015) Degradation of p-nitrophenol by heat and metal ions co-activated persulfate. Chem Eng J 264:39–47